N O T I C E

THIS DOCUMENT HAS BEEN REPRODUCED FROM MICROFICHE. ALTHOUGH IT IS RECOGNIZED THAT CERTAIN PORTIONS ARE ILLEGIBLE, IT IS BEING RELEASED IN THE INTEREST OF MAKING AVAILABLE AS MUCH INFORMATION AS POSSIBLE

NASA Technical Memorandum 81553

(NASA-TM-81553) NUMERICAL TECHNIQUES IN LINEAR DUCT ACOUSTICS Status Report (NASA) 23 p HC A02/MF A01 CSCL 20A

N80-30154

Unclas

G3/71 28453

NUMERICAL TECHNIQUES IN LINEAR DUCT ACOUSTICS – A STATUS REPORT

K. J. Baumeister
Lewis Research Center
Cleveland, Ohio

Prepared for the
Winter Annual Meeting of the American
Society of Mechanical Engineers
Chicago, Illinois, November 17-21, 1980

SEP 1980
RECEIVED
NASA STI FACILITY
ACCESS DEPT.

NASA

NUMERICAL TECHNIQUES IN LINEAR DUCT ACOUSTICS - A STATUS REPORT

by

K. J. Baumeister
NASA Lewis Research Center
Cleveland, Ohio

ABSTRACT

A review is presented covering both finite difference and finite element analysis of small amplitude (linear) sound propagation in straight and variable area ducts with flow, as might be found in a typical turbojet engine duct, muffler, or industrial ventilation system. Both "steady" state and transient theories are discussed. Emphasis is placed on the advantages and limitations associated with the various numerical techniques. Examples of practical problems are given for which the numerical techniques have been applied.

E-513

NOMENCLATURE

A	matrix, Eq. (54)
a_k	cell coefficient, Eq. (53)
b_k	cell coefficient, Eq. (53)
C_k	cell coefficient, Eq. (53)
C_o^*	ambient speed of sound, m/s
$\overline{C}^2$	$1 - (\gamma - 1)/2 \left[\phi_r^2 + \phi_x^2\right]$
d_k	cell coefficient, Eq. (53)
d_o^*	duct diameter
E	total number of elements
e	element
e_k	cell coefficient, Eq. (53)
F	initial condition vector, Eq. (54)
f^*	frequency, Hz
f	function of y, see Eq. (39)
H^*	duct height, m
I	number of axial grid points
i	$\sqrt{-1}$
J	number of transverse grid points
k	number of time steps
L^*	length of duct, m
m	spinning mode number
N	total number of finite element nodes
N_{Grid}	number of grid points
N_n^e	element interpolation function for node n
N_{sub}	number of storage locations in sub matrix
n	node number in finite element analysis
n_t	transverse mode number
P^*	pressure, N/m^2
P	time dependent acoustic pressure, $P^*/\rho_o^* C_o^{*2}$
P_m^*	acoustic pressure, $P_m^*(t,x,r)$, Eq. (12), N/m^2
P_o^*	mean flow pressure, N/m^2
P_1^*	fluctuating acoustic pressure, N/m^2
p	spatially dependent acoustic pressure
p_o	wave envelope pressure, Eq. (62)
R^*	gas constant, m^2/sec^2 K
r	radius dimensionless, r/r_o^*
r_o^*	radius of duct
Δr	radial grid spacing

T^*	temperature, K
T_o^*	mean field temperature, K
T_1^*	fluctuation acoustic temperature, K
t	dimensionless time, t^*/t_p^*
t_p	period $1/f^*$, sec
Δt	time step
U	time dependent axial dimensionless acoustic velocity, $U(x,y,t)$, U^*/C_o^*
U_o	dimensionless mean flow velocity in axial direction, U_o^*/C_o^*
u	spatial dimensionless axial acoustic velocity $u(x,y)$
V	time dependent dimensionless transverse or radial dimensionless acoustic velocity, $V(x,y,t)$
$\vec{V}^*$	vector flow velocity, m/sec
$\vec{V}_o^*$	mean vector flow velocity, m/sec
$\vec{V}_1^*$	fluctuating vector flow velocity, m/sec
v	spatial dimensionless transverse or radial dimensionless acoustic velocity,
W	time dependent dimensionless acoustic velocity in θ direction, $W(x,r,\theta,t)$
w	spatial dimensionless acoustic velocity in direction, $w(x,r,\theta)$
x	axial coordinate, x^*/H^* or x^*/r_o^*
x_m	mapped axial coordinates
Δx	axial grid spacing
y	dimensionless transverse coordinate, y^*/H^*
y_m	mapped transverse coordinate
Δy	transverse grid spacing
Z^*	impedance, kg/m^2 sec
γ	ratio of specific heats
ζ	specific acoustic impedance
η	dimensionless frequency, $H^*/f^*/C_o^*$ (cartesian) or $r_o^*f^*/C_o^*$ (cylindrical)
λ	dimensionless wave length
θ	angle, radians
θ_r	dimensionless specific resistance
ρ	dimensionless acoustic density fluctuation, ρ^*/ρ_o^*
ρ^*	density, kg/m^3
ρ_o^*	ambient air density, kg/m^3
ρ_1^*	fluctuation acoustic density, kg/m^3
ϕ_o^*	flow potential function, m^2/sec
ϕ^*	mean flow potential function, m^2/sec
ϕ	dimensionless acoustic potential function, $\phi^*/C_o^*d_o^*$
ϕ^*	spatial acoustic potential function, m^2/sec
ϕ_1^*	fluctuation velocity potential function, m^2/sec
χ	dimensionless reactance
ω	angular frequency, $\omega^*d_o^*/C_o^*$
ω^*	angular frequency

SUBSCRIPTS

e	exit condition
i	axial index (fig. 2)
j	transverse index (fig. 2)
o	ambient condition or mean flow variables
s	spatial value
t	transient
1	fluctuation quantity

SUPERSCRIPTS

*	dimensional quantity
k	time step index
(1)	real part
(2)	imaginary part
$(\vec{\ })$	vector quantity

INTRODUCTION

With the introduction of strict aircraft noise regulations in the late 1960's, the new aircraft nacelle designs required acoustic treatment in the inlet and exhaust ducts to reduce engine fan noise. To minimize the weight penalty of wall treatment, the aerospace industry has been concerned with reducing

the length of a liner for a required sound attenuation. To perform this optimization, sophisticated and flexible suppressor analytical techniques are needed to handle sound propagation in ducts with axial variations in cross-sectional area, wall liner impedance (absorbers), and with gradients in the flow Mach number. In an attempt to meet this need, both finite difference and finite element techniques were developed. In a parallel effort, universities and industry have also developed similar numerical programs to analyze acoustic propagation in mufflers and ventilation systems.

In this paper, a review is presented covering both finite difference and finite element analysis of small amplitude (linear) sound propagation in straight and variable area ducts with and without flow. Both "steady" state and transient theory will be discussed. In the "steady" state theory, the pressure and acoustic velocities are assumed to be simple harmonic functions of time; thus, the governing linearized gas-dynamic equations become independent of time.

The numerical analysis to be considered employs a full two or three dimensional finite difference or finite element theory. The theories to be discussed will have provision for inlet and outlet flow, such as in a muffler or jet engine duct.

Application of finite difference or finite elements to acoustic propagation in enclosed rooms (refs. 1-8) or to coupled structural-acoustic radiation systems (refs. 9-12) will not be included. Also, theories will not be covered which use the finite difference analysis to determine the eigenvalue and corresponding modal pressure difference across the duct (refs. 13-17). These works have been included in the list of reference for completness.

First, the equations governing sound propagation are presented along with the boundary and initial conditions associated with a typical turbojet engine duct. Next, the various numerical theories developed in the literature are presented in the following order:

(1) Steady State Finite Difference Theory
(2) Steady State Finite Element Theory
(3) Special Numerical Transformations
(4) Transient Numerical Theory

Items (3) and (4) represent special attempts to eliminate the problems associated with the highly oscillatory nature of sound propagation in the inlet of a turbojet engine.

GOVERNING EQUATIONS

In this section, the general fluid flow equations will first be introduced in vector form. From these equations, the general linearized gas-dynamic equations, which govern the propagation of sound down a duct, will be developed. These equations will be specialized to the case of a parallel shear flow in a duct with uniform mean temperature and pressure. Next, the parallel shear flow equations will be written for cylindrical and cartesian coordinates. Finally, the equations will also be presented in terms of the velocity potential.

Unsteady Invisid Flow

The basic equations governing sound flow in air ducts are the usual continuity, inviscid momentum (Euler), energy, and equation of state. In the absence of any external sources of mass or momentum, and neglecting viscosity and heat transfer, these equations are:

Continuity $$\frac{\partial \rho^*}{\partial t^*} + \nabla^* \cdot (\rho^* \vec{V}^*) = 0 \tag{1}$$

Momentum $$\rho^* \left(\frac{\partial \vec{V}^*}{\partial t^*} + \vec{V}^* \cdot \nabla^* \vec{V}^* \right) = - \nabla^* P^* \tag{2}$$

Energy $$\frac{\partial \rho^*}{\partial t^*} + \vec{V}^* \cdot \nabla^* \rho^* = \frac{1}{C^{*2}} \left(\frac{\partial P^*}{\partial t^*} + \vec{V}^* \cdot \nabla^* P^* \right) \tag{3}$$

State $$P^*/\rho^* = R^* T^* \tag{4}$$

Where an asterisk denotes dimensional quantities.

Linearized Gas-Dynamic Equations

Customarily, the dependent flow parameters ρ^*, V^*, and P^* are represented as the sum of a mean quantity and a small fluctuating quantity, i.e. $\rho^* = \rho_o^* + \rho_1^*$, $T^* = T_o^* + T_1^*$, $\vec{V}^* = \vec{V}_o^* + \vec{V}_1^*$ and $P^* = P_o^* + P_1^*$ where the subscript o represents the mean component and 1 represents the fluctuating component. The mean flow quantities are assured independent of time and thereby satisfy the steady mean flow equation. Substituting these assumed expressions into Eqs. (1) to (4), eliminating the mean flow quantities and neglecting nonlinear acoustic quantities yields:

Continuity $$\frac{\partial \rho_1^*}{\partial t^*} + \nabla^* \cdot (\rho_o^* \vec{V}_1^* + \rho_1^* \vec{V}_o^*) = 0 \tag{5}$$

Momentum $$\rho_o^* \left(\frac{\partial \vec{V}_1^*}{\partial t^*} + \vec{V}_o^* \cdot \nabla^* \vec{V}_1^* + \vec{V}_1^* \cdot \nabla^* \vec{V}_o^* \right) + \rho_1^* \vec{V}_o^* \cdot \nabla^* \vec{V}_o^* = - \nabla^* P_1^* \tag{6}$$

Energy $$C_o^{*2} \left(\frac{\partial \rho_1^*}{\partial t^*} + \vec{V}_o^* \cdot \nabla^* \rho_1^* + \vec{V}_1^* \cdot \nabla^* \rho_o^* \right) + C_1^{*2} \vec{V}_o^* \cdot \nabla^* \rho_o^* = \frac{\partial P_1^*}{\partial t^*} + \vec{V}_o^* \cdot \nabla^* P_1^* + \vec{V}_1^* \cdot \nabla^* P_o^* \tag{7}$$

State $$\frac{P_1^*}{P_o^*} = \frac{\rho_1^*}{\rho_o^*} + \frac{T_1^*}{T_o^*} \tag{8}$$

The vector form of Eqs. (5) to (7) were listed by Goldstein (ref. 18, p. 5). These equations are frequently referred to as the linearized gas-dynamic equations.

For the special and important case where the mean velocity remains constant and parallel to the duct walls (parallel shear flow) and for which the mean flow temperature and pressure are constants, the energy Eq. (7) reduces to:

$$P_1^* = C_o^{*2} \rho_1^* \tag{9}$$

This derivation is most easily accomplished by first expressing the energy equation in terms of entropy (ref. 18, p. 8). The linearized continuity and momentum equations become:

$$\frac{\partial P_1^*}{\partial t^*} + C_o^{*2} \rho_o^* \nabla^* \cdot \vec{V}_1^* + \nabla^* \cdot P_1^* \vec{V}_o^* = 0 \tag{10}$$

$$\rho_o^*\left(\frac{\partial \vec{V}_1^*}{\partial t^*} + \vec{V}_o^* \cdot \nabla^* \vec{V}_1^* + \vec{V}_1^* \cdot \nabla^* \vec{V}_o^*\right) = -\nabla^* P_1^* \qquad (11)$$

(Parallel shear flow)

Cylindrical Coordinates

Figure 1 shows the typical ducting for a turbofan engine. Noise from the fan travels up the circular inlet against the flow and down through the annular exhaust duct as shown. Thus, a cylindrical coordinate system (x,r,θ) is appropriate for the analysis. In general, the acoustic field is three dimensional. The sound variation in the axial x direction will depend on frequency, duct area, and be very large in the presence of wall absorbers. The acoustic field may also vary radially from the hub to tip at the rotor (see fig. 1). Because of the rotation of the rotor blades, large circumferential variations (see fig. 1) in acoustic pressure may also occur depending on blade number and engine rpm.

A three dimensional solution for sound propagation would be expensive to perform. Customarily, since the equations are linear, the circumferential acoustic pressure and velocity variations are decomposed into spinning modes m:

$$P_1^*(x,r,\theta,t) = \sum_m P_m^*(x,r,t)e^{im\theta} \qquad (12)$$

The summation is over those lobe numbers (m) that are likely to occur in a particular application. Using the assumption that

$$P_1^* \text{ and } V_1^* \sim e^{im\theta} \qquad (13)$$

Equations (10) and (11) for parallel shear flow in cylindrical coordinates become after nondimensionalizing

$$\frac{\partial P}{\partial t} = -\frac{1}{\eta}\frac{\partial U}{\partial x} - \frac{1}{\eta}\frac{\partial V}{\partial r} - \frac{im}{r\eta}W - \frac{V}{\eta r} - \frac{U_o}{\eta}\frac{\partial P}{\partial x} \qquad (14)$$

$$\frac{\partial U}{\partial t} = -\frac{1}{\eta}\frac{\partial P}{\partial x} - \frac{U_o}{\eta}\frac{\partial U}{\partial x} - \frac{1}{\eta}\frac{\partial U_o}{\partial r}V \qquad (15)$$

$$\frac{\partial V}{\partial t} = -\frac{1}{\eta}\frac{\partial P}{\partial r} - \frac{U_o}{\eta}\frac{\partial V}{\partial x} \qquad (16)$$

$$\frac{\partial W}{\partial t} = -\frac{im}{\eta r}P - \frac{U_o}{\eta}\frac{\partial W}{\partial x} \qquad (17)$$

Equations (14) to (17) are in dimensionless form, where the particular nondimensionalizing variables are tabulated in the list of symbols. The dimensionless frequency η based on the radius of the duct is given by

$$\eta = \frac{\omega^*}{2\pi}\frac{r_o^*}{C_o^*}$$

$$\left(\text{or } \frac{f^* H^*}{C_o^*} \text{ for cartesian coordinates to be used later}\right) \qquad (18)$$

Equations (14) to (17) will combine to yield a third order partial differential equation in pressure, as shown by Savkar (ref. 19). In the absence of shear $\left(\frac{\partial U_o}{\partial r} = 0\right)$, Eqs. (14) to (17) combine into the usual plug flow wave equation

$$\eta^2\frac{\partial^2 p}{\partial t^2} = (1 - U_o^2)\frac{\partial^2 p}{\partial x^2} + \frac{\partial^2 p}{\partial r^2} - \frac{m^2}{r^2}p - 2\eta U_o\frac{\partial^2 p}{\partial t\partial x} + \frac{1}{r}\frac{\partial p}{\partial r} \qquad (19)$$

In the steady state analysis, the noise source and dependent acoustic parameters are always assumed to be of the form

$$P_1^* \text{ or } V_1^* \sim e^{i\omega^* t^*} = e^{i2\pi t} \qquad (20)$$

Consequently, Eqs. (14) to (17) and Eq. (19) reduce to

$$(i2\pi\eta)p = -\frac{\partial u}{\partial x} - \frac{\partial v}{\partial r} - \frac{im}{r}w - \frac{v}{r} - U_o\frac{\partial p}{\partial x} \qquad (21)$$

$$(i2\pi\eta)u = -\frac{\partial p}{\partial x} - U_o\frac{\partial u}{\partial x} - \frac{\partial U_o}{\partial r}v \qquad (22)$$

$$(i2\pi\eta)v = -\frac{\partial p}{\partial y} - U_o\frac{\partial v}{\partial x} \qquad (23)$$

$$(i2\pi\eta)w = -\frac{im}{r}p - U_o\frac{\partial w}{\partial x} \qquad (24)$$

$$(2\pi\eta)^2 p = (1 - U_o^2)\frac{\partial^2 p}{\partial x^2} + \frac{\partial^2 p}{\partial r^2} - \frac{m^2}{r^2}p - i4\pi\eta U_o\frac{\partial p}{\partial x} + \frac{1}{r}\frac{\partial p}{\partial r} \qquad (25)$$

The acoustic variables shown in lower case represent the time independent values.

Cartesian Coordinates

The annular exit duct in the turbojet engine can be represented approximately by rectangular geometry. Also, many experiments are performed in rectangular geometries. For simplicity, spinning modes have been neglected. In the absence of spinning modes, the rectangular forms of the governing equations are

$$\frac{\partial P}{\partial t} = -\frac{1}{\eta}\frac{\partial U}{\partial x} - \frac{1}{\eta}\frac{\partial V}{\partial y} - \frac{U_o}{\eta}\frac{\partial P}{\partial x} \qquad (26)$$

$$\frac{\partial U}{\partial t} = -\frac{1}{\eta}\frac{\partial P}{\partial x} - \frac{U_o}{\eta}\frac{\partial U}{\partial x} - \frac{1}{\eta}\frac{\partial U_o}{\partial y}V \qquad (27)$$

$$\frac{\partial V}{\partial t} = -\frac{1}{\eta}\frac{\partial P}{\partial y} - \frac{U_o}{\eta}\frac{\partial V}{\partial x} \qquad (28)$$

Likewise, the steady state equations (using eq. (20)) become

$$(i2\pi\eta)p = -\frac{\partial u}{\partial x} - \frac{\partial v}{\partial y} - U_o\frac{\partial p}{\partial x} \qquad (29)$$

$$(i2\pi\eta)u = -\frac{\partial p}{\partial x} - U_o\frac{\partial u}{\partial x} - \frac{\partial U_o}{\partial y}v \qquad (30)$$

$$(i2\pi\eta)v = -\frac{\partial p}{\partial y} - U_o\frac{\partial v}{\partial x} \qquad (31)$$

For the case of no shear $\left(\frac{\partial U_o}{\partial y} = 0\right)$, Eqs. (26) to (28) combine into a single second order wave equation

$$\eta^2 \frac{\partial^2 p}{\partial t^2} = (1 - U_o^2) \frac{\partial^2 p}{\partial x^2} + \frac{\partial^2 p}{\partial y^2} - 2\eta U_o \frac{\partial^2 p}{\partial t \partial x} \tag{32}$$

The steady state form of Eq. (32) becomes

$$(1 - U_o^2) \frac{\partial^2 p}{\partial x^2} + \frac{\partial^2 p}{\partial y^2} - i4\pi\eta U_o \frac{\partial P}{\partial x} + (2\pi\eta)^2 P = 0 \tag{33}$$

In the absence of flow (U_o equals zero) Eq. (33) reduces to the classic Helmholtz equation

$$\frac{\partial^2 p}{\partial x^2} + \frac{\partial^2 p}{\partial y^2} + (2\pi\eta)^2 p = 0 \tag{34}$$

Potential Flow Equations

When using numerical techniques in calculating sound propagating in ducts, the velocity potential formulation of the acoustic wave equation offers many advantages over the conventional linearized gas equations. For three dimensional flows, the velocity potential approach reduces the computer storage and running time by an order of magnitude compared to the more general linearlized gas equation approach, because only one dependent variable ϕ is required. Since the flow into the inlet is usually modelled by potential flow (excluding the boundary layer), the acoustic velocity potential is ideally suited for acoustic inlet calculations. Sigman, Majjigi and Zinn (ref. 20) give the potential gas-dynamic equations for a cylindrical duct. The general velocity potential equation for inviscid flow (ref. 16, eq. (1))

$$\frac{\partial^2 \bar{\Phi}^*}{\partial t^{*2}} + \frac{\partial}{\partial t^*} (\nabla^* \bar{\Phi}^* \cdot \nabla^* \bar{\Phi}^*)$$

$$+ \frac{1}{2} \nabla^* \bar{\Phi}^* \cdot \nabla^* (\nabla^* \bar{\Phi}^* \cdot \nabla^* \bar{\Phi}^*) - C^{*2} \nabla^{*2} \bar{\Phi}^* = 0 \tag{35}$$

was the starting point for their analysis. First, they assumed

$$\bar{\Phi}^* = \Phi^* + \phi_1^* \tag{36}$$

where again the symbol Φ^* represents the steady mean value of the velocity potential and ϕ_1^* the fluctuation quantity. Next, because the fan generates spinning acoustic modes, they assumed

$$\phi_1^*(x,r,\theta,t) = \phi^*(x,r) e^{-i\omega t} e^{im\theta} \tag{37}$$

Substituting Eqs. (36) and (37) into Eq. (35), yields (dimensionless)

$$L(\phi) = (\bar{C}^2 - \phi_r^2)\phi_{rr} + (\bar{C}^2 - \phi_x^2)\phi_{xx} - 2\phi_r\phi_x\phi_{rx}$$

$$+ \left[- (\gamma + 1)\phi_{rr}\phi_r - 2\phi_x\phi_{rx} + \frac{\bar{C}^2}{r} - (\gamma - 1) \frac{1}{r} \phi_r^2\right.$$

$$\left. - (\gamma - 1)\phi_r\phi_{xx}\right] \phi_r + \left[- (\gamma + 1)\phi_{xx}\phi_x - 2\phi_{rx}\phi_r\right.$$

$$\left. - (\gamma - 1)\phi_{rr}\phi_x - (\gamma - 1) \frac{1}{r} \phi_r\phi_x\right] \phi_x$$

$$+ [\omega^2 - m^2 \bar{C}^2/r^2]\phi + i2\omega\phi_r\phi_r + i2\omega\phi_x\phi_x$$

$$+ i\omega(\gamma - 1)\left[\phi_{rr} + \frac{1}{r} \phi_r + \phi_{xx}\right]\phi = 0 \tag{38}$$

BOUNDARY CONDITIONS

To obtain a solution to the previously developed equations, boundary conditions are required at the liner entrance, duct liner walls, and exit plane.

Entrance Condition

For a rectangular duct, the boundary condition at the liner entrance $P(o,y,t)$ can be of form

$$P(o,y,t) = f(y) e^{i\omega^* t^*} \tag{39}$$

where $f(y)$ represents the transverse variation in pressure. Similar expressions for ϕ or acoustic velocity can be used. In cylindrical coordinates, the radial coordinate r would replace y in Eq. (39). In a rectangular duct, spatial pressure variations at the liner entrance $f(y)$ have been taken to be plane ($f = 1$) or some harmonic $\left(\cos\left[n_t \pi y\right]\right)$ associated with the normal-mode analytical solutions (ref. 21, p. 504). In cylindrical ducts, the spatial variations in the radial direction are of the form of Bessel functions (ref. 21, p. 511).

Physically, boundary condition (39) represents the sum of a forward and reflected acoustic wave at $x = o$. In a uniquely different approach, Eversman et al. (ref. 22) assume an infinite duct upstream of the source, and that Eq. (39) represents only the forward propagating wave. Their analysis separates the reflected and transmitted waves. At the present time, both approaches to the entrance conditions are used in modelling the sound input into the acoustic suppressor.

Wall Boundary Conditions

The boundary condition at the surface of a locally reacting sound absorbant soft-wall duct can be expressed in terms of a specific acoustic impedance defined as the ratio of pressure to transverse acoustic velocity:

$$\zeta = \frac{Z^*}{\rho_o^* C_o^*} = \frac{P}{V} = \frac{P}{v} \tag{40}$$

For shear flow, the mean velocity at the wall is zero; therefore, substituting Eq. (40) into Eq. (28) yields

$$\frac{\partial P}{\partial y} = - \frac{n}{\zeta} \frac{\partial P}{\partial t} \tag{41}$$

For harmonic excitation, $e^{i\omega^* t^*}$, Eq. (41) reduces to

$$\frac{\partial p}{\partial y} = -\frac{i2\pi\eta}{\zeta} p \tag{42}$$

Equations (41) and (42) are useful when working with the wave equation formulated in terms of only pressure. Equation (40) is more useful when solving the continuity and momentum equations simultaneously.

It is also convenient to express the specific acoustic impedance in terms of resistance θ_r and reactance χ as

$$\zeta = \theta_r + i\chi \tag{43}$$

Exit Impedance

In a manner similar to the wall impedance, the axial impedance at the duct exit can be defined as

$$\zeta_e = \frac{P(L^*/H^*,y,t)}{U(L^*/H^*,y,t)} \tag{44}$$

General values for the exit impedance for single modes can be found in references 20 or 23. As with the source condition, Eversman, et al. (ref. 22) use the technique of accounting for reflected and transmitted waves. For arbitrary multi-modal wave forms, however, a general impedance equation is not available for use in the numerical techniques.

Initial Conditions

In the transient analysis, for times equal or less than zero, the duct is assumed quiescent, that is, the acoustic pressure and velocities are taken to be zero. For times greater than zero, the application of the noise source (eq. (39)) will drive the pressures in the duct.

STEADY STATE FINITE DIFFERENCE THEORY

In 1973, Alfredson (ref. 24) and Baumeister and Bittner (ref. 25) presented a finite difference theory for noise propagation in both hard and soft wall ducts in the absence of flow. In the 1973 Aero-Acoustic conference, Baumeister and Rice (ref. 26) simulated noise propagation in the jet engine duct by including mean flow with the finite difference theory.

In the first step of these finite difference analyses, the continuous acoustic flow field is lumped into a series of grid points for which discrete values of the acoustic pressure are defined, as shown in Fig. 2 for a rectangular duct.

Grid Point Requirements

The question naturally arises as to how many grid points are required in the axial (x) direction and the transverse (y) direction to obtain reasonably accurate results. The following one-dimensional analysis will be helpful in determining the required number of grid points. For the special case of plane wave propagation in a hard wall duct, no pressure gradients will exist in the transverse direction in the duct; consequently, the wave Eq. (33) reduces to the one dimensional form

$$(1 - U_o^2)\frac{\partial^2 p}{\partial x^2} - i4\pi\eta U_o \frac{\partial p}{\partial x} + (2\pi\eta)^2 p = 0 \tag{45}$$

For a semi-infinite duct (no reflections), the solution to Eq. (45) for the complex acoustic pressure is

$$p = e^{-i\frac{2\pi\eta x}{1+U_o}} \tag{46}$$

Thus, the pressure oscillates down the duct with a wave length

$$\lambda = \frac{1 + U_o}{\eta} \tag{47}$$

The real part of the acoustic pressure in Eq. (46) is shown in Fig. 3 for the case of a dimensionless frequency $\eta = 5$ and a zero Mach number. Five separate oscillations appear in the duct. If a Mach number U_o of -0.5 is introduced to simulate the inlet flow of a turbofan engine, Eq. (47) indicates that the wave length would decrease by half, and ten full oscillations would appear in the duct. In a detailed study of the accuracy of the numerical solutions to this problem, Baumeister and Bittner (ref. 25) showed that at least twelve grid points per wavelength are required to accurately resolve the pressure and the transmitted acoustic power. Thus, the number of grid points required in the axial direction is

$$I \geq \frac{12\, L^*/H^*\, \eta}{1 + U_o} \tag{48}$$

Besides the axial acoustic oscillations, transferse acoustic oscillations (ref. 21, p. 492) can also exist in the duct. In a recent paper, Baumeister (ref. 27) showed that the number of grid points J in the transverse direction required to accurately resolve the highest order propagating mode is

$$J \geq 12\,\eta \tag{49}$$

Thus, the total number of grid points N_{Grid} required in the duct is the product of Eqs. (48) and (49):

$$N_{Grid} = \frac{144\,\eta^2 L^*/H^*}{1 + U_o} \tag{50}$$

Although a large number of grid points is required particularly at high frequencies, a more difficult problem results from the nature of the governing steady state acoustic equations themselves, as will be considered next.

Difference Equation

The continuous governing differential equations can be changed to a system of algebraic equations by means of the finite difference approximations. This set of algebraic equations can then be solved simultaneously to determine the pressure at each grid point. In constructing the difference equations, only sound propagation in the absence of flow will be developed here in order to keep the mathematics simple.

Without flow, the classic Helmholtz equation (eq. (34)), governs pressure propagation in the duct. Using the usual 5 point difference approximations, Eq. (34) becomes

$$\left(\frac{p_{i-1,j} - 2p_{i,j} + p_{i+1,j}}{\Delta x^2}\right) + \left(\frac{p_{i,j-1} - 2p_{i,j} + p_{i,j+1}}{\Delta y^2}\right) + (2\pi\eta)^2 p_{i,j} = 0 \tag{51}$$

or for Δx equal to Δy

$$p_{i-1,j} + p_{i,j-1} - [4 - (2\pi n\Delta x)^2] p_{i,j} + p_{i,j+1} + p_{i+1,j} = 0 \tag{52}$$

Equation (52) applies only to cell 1 in Fig. 2 which is not adjacent to the boundaries. For the other cells in Fig. 2, a complex impedance condition is specified along a boundary. The integration method is most convenient to use for generating the difference equations at the boundaries, as fully documented in Ref. 28, Appendix D.

The finite-difference approximations for the various cells shown in Fig. 2 can be expressed in terms of the coefficients

$$a_k p_{i-1,j} + b_k p_{i,j-1} + c_k p_{i,j} + d_k p_{i,j+1} + e_k p_{i+1,j} = 0 \tag{53}$$

The subscript k denotes the cell number. The collection of the various difference equations at each grid point forms a set of simultaneous equations that can be expressed as

$$\{A\}[P] = [F] \tag{54}$$

where $\{A\}$ is the known coefficient matrix, $[P]$ is the unknown pressure vector, and $[F]$ is the known column vector containing the various boundary conditions. The matrix is complex because of the complex nature of the source and impedance boundary conditions.

Matrix Solution

The magnitude of the frequency term $(2\pi n\Delta x)^2$ in Eq. (52), which subtracts from the main diagonal element c_k of coefficient matrix represented by Eq. (54), is such that the matrix is not diagonally dominant. As a result, iteration solutions cannot be used. Equation (54) is usually solved by the Gauss elimination technique. In general, the elimination technique requires the storage of all the matrix elements which would be represented by twice (complex nature) the square of N_{Grid} given by Eq. (50). For high frequencies (η), this represents a large burden on the storage capacity of a computer. Sparse-matrix techniques (ref. 29) have been employed to reduce computer storage and run times as much as possible. Quinn (ref. 29) partitioned the matrix $\{A\}$ into a tridiagonal form, which reduced the elements in the submatrix to

$$N_{sub} = J^2 = 144\ \eta^2 \tag{55}$$

Quinn's program stores the elements of the submatrices in separate locations on tape or disk. These matrices are then read in one at a time to obtain a solution of the matrix.

Baumeister (ref. 27) and Quinn (ref. 30) have modified similar matrixes to allow iteration techniques; unfortunately, the convergence is too slow to be of any practical value. Other approaches, such as in Ref. 31, might still offer iterative possibilities.

Example Solutions

Figure 4 shows some sample numerical calculations for a plane wave propagating in a uniform hard wall duct. As seen in Fig. 4, the numerical theory and exact analysis are in good agreement.

Area Variations

So far in this paper, the difference theory considered only straight uniform area ducts. Generally, finite differences when applied to irregular ducts requires considerable bookkeeping (ref. 32, p. 363). Quinn (refs. 33 and 34), however, applied the method of conformal mapping in conjunction with finite differences to analyze sound propagation in a hyperbolic horn shown in Fig. 5. In the absence of flow, the following transformations

$$x = \frac{e^{x_m} - e^{-x_m}}{2} \cos y_m \tag{56}$$

$$y = \frac{e^{x_m} + e^{-x_m}}{2} \sin y_m \tag{57}$$

change the governing Helmholtz equation into

$$\frac{\partial^2 p}{\partial x_m^2} + \frac{\partial^2 p}{\partial y_m^2} + (2\pi\eta)^2 F(x_m, y_m) p = 0 \tag{58}$$

where

$$F(x_m, y_m) = \frac{e^{2x_m} - e^{-2x_m} + 2(\cos^2 y_m - \sin^2 y_m)}{4} \tag{59}$$

Equation (58) was programmed in finite difference form by Quinn for the straight duct shown in Fig. 5. Quinn also conformally mapped a conical horn and found the numerical results to be in excellent agreement with known analytical solutions.

In general, for ducts with variable area, the finite element theory is the most convenient to use. However, as pointed out by Quinn (ref. 30), the advantage of finite elements versus finite differences is not as great when a mapping function is used to compute the mean flow field. For example, conformal mapping has been used in the calculation of subsonic and transonic inlet flow fields in the DC-8 engine (ref. 35). In such a case, where the conformal transformation is available, the use of finite difference theory would clearly have an advantage over finite element theory.

STEADY STATE FINITE ELEMENT THEORY

The use of finite element techniques in duct acoustics began in 1975. Young and Crocker (ref. 36) developed a two-dimensional finite element solution of acoustic propagation in mufflers without flow using a variational technique. In a preliminary investigation, Kapur and Mungur (ref. 37) concluded that a finite element Galerkin method could be successfully employed to handle shear flow in ducts with area variations. Since these papers, numerous finite element solutions of the duct propagation problem have appeared in the literature and will be discussed herein. First, however, a brief review of the finite element theory is presented to establish categories to classify the various references in the acoustic literature.

Basic Theory

The solution of the duct acoustic problem by the finite element theory follows the usual step-by-step process (ref. 38, p. 7) developed for any continuum problem. These steps will now be succinctly listed with particular emphasis on how they relate to the duct acoustic problem.

1. Discretize the Continuum: The first step is to divide the interior of the duct into elements. A variety of elements have been used in the duct acoustic problem as shown in the first column of Table I. Table I will be used as a focal point about which the discussion of the acoustic literature will center.

2. Select Interpolation Function: The next step is to assign nodes to the element and then choose the type of interpolation function to represent the variation inside the elements of the field variable, such as pressure and the acoustic velocities. In Table I, column two shows the node pattern while column three describes the interpolation function. The required number of elements can be estimated from the results of the finite difference theory. For sound propagation without large reflections (exclude low frequency as in mufflers), Eq. (50) can be used to estimate the number of finite elements necessary to obtain an accurate solution. In determining the required number of finite elements, however, the constant 144 will be smaller because the interpolation function in finite element theory is generally of higher order than the first order linear difference approximation used to establish Eq. (50). The precise decrease will depend on the type of element used in the analysis. In general, the more nodes per element the fewer will be the number of elements needed to resolve the acoustic field. On the other hand, since the size of the solution (global) matrix is proportional to the number of nodes, considerably more computational time and computer core memory are required for the higher order elements. Column four lists the number of dependent variables considered in the particular study. For a fixed number of elements, the computer storage will be proportional to the square of the number of dependent variables while the solution times can increase by the cube (ref. 39, p. 261) of the dependent variables. Clearly, those equations should be employed which can successfully model the physics with the fewest dependent variables.

Generally, Lagrange polynominals are used for interpolation when only one field variable (such as pressure p) is calculated at each node, commonly called the C^0 continuity problem. When using Hermite polynominals, the values of $\partial p/\partial x$ and $\partial p/\partial y$ can also be calculated at each node, commonly called the C^1 problem. In general, C^1 continuity is more difficult to construct (ref. 38, p. 172), so with the exception of items 1 and 5 in Table I, Lagrange polynominals are used. Also, if C^1 continuity increases the unknowns by four (item 5, Table I), then the resulting solution matrix will increase by about sixteen.

3. Finite Element Method: Next, the unknown nodal values of the pressure (or any other dependent variable) must now be constrained such that the nodal pressures provide an accurate approximation for the true pressure distribution. In conjunction with the governing differential equations and boundary conditions, a finite element method is used to develop the algebraic element equations for the unknown pressures associated with each element. The element equations are then combined into a general matrix (global) which is solved for the pressures at the nodes.

In acoustics, except for the no flow case, the Galerkin finite element method is most often used to establish the matrix equations for the unknown field variable. For example, consider the case using the velocity potential to describe the acoustic field, Eq. (38). Application of the Galerkin Finite element method yields the following relationship

$$\sum_{e=1}^{E} \iint N_m^e L(\phi)\, dA^{(e)} = 0 \qquad n = 1,2,\ldots N \tag{60}$$

where the integration is performed over the area of each element. The known interpolation function N_n^e is for the n node in the e th element and N is the total number of nodes in the problem under consideration. It should be noted that N_n^e is zero for all elements not having the nodal point as a vertex. Equation (60) provides N equations for the N unknown nodal values.

4. Matrix Equations: To find the solution to the complete network of elements, all the element equations must now be assembled into a global matrix. With the exception of the least squares approach, the solutions are all accomplished by some sort of elimination procedure. Effective solutions take into account the banded nature of the matrix. The band width increases with a larger number of element nodes and number of dependent variables. As with finite difference, the storage requirement of the finite element solution can severely restrict the range of problem that can be solved as pointed out by Quinn (ref. 30). For the larger problems, an out-of-core banded solver is generally required with a moderate amount of in-core storage but much more input/output time.

Finite Element Theories

The following discussions of the published finite element theories will be in order of the complexity of the flow field and interpolation function and not chronological.

No Flow. Young and Crocker (ref. 36, item 1, Table I) developed a two-dimensional finite element model for analyzing sound propagation in expansion chambers with hard walls. The basic elements were rectangles using one-dimensional Hermitian polynominals of fourth order. Good agreement was found between the finite-element approach and the acoustic filter theory at low frequencies where plane wave analysis applies. At the higher frequencies, where the diameter to wave length ratio is greater than 0.8, significant differences between the plane wave and the two-dimensional finite element analysis were found.

Kagama and Omote (ref. 40, item 2, Table I) expanded the analytical work of Young and Crocker to lined axisymmetric soft wall mufflers with more complicated inputs. A linear three node triangular element was used in Ref. 40 for the hard wall muffler while a six node element triangle was used in Ref. 41, item 3, Table I, in the soft wall analysis. A wealth of example problems were considered in these papers. Rectangular and conical mufflers were analyzed with

and without sound absorbing materials. Significantly, experimental data were obtained for all the examples analyzed. Excellent agreement between the finite element theory and experiments was obtained. Therefore, the acoustic response of a muffler of any shape can be accurately and easily determined by a two-dimensional finite element analysis. In the same time frame, Craggs (refs. 42 and 43) presented a formulation and approach similar to that of Kagawa and Omute. Craggs used a more refined axisymmetric hexahedral isoparametric element as shown in Table I, item 4. Isoparametric elements allows the sides of the hexahedral element to bend and more closely match the shape of a curved boundary. In Refs. 44 and 45, Craggs extended his treatment of sound absorbing materials to include extended reaction effects. His two-dimensional model showed that propagation parallel to the incident boundary can be important

Tag, Lumsdaine, and Akin (refs. 46 and 47) have applied linear rectangular isoparametric elements to two-dimensional (cartesian) rectangular ducts with soft walls without flow. Examples are shown (ref. 46) for sound propagation around circular and rectangular bends as might commonly be seen in industrial ducts. Some simple plane wave propagation examples with plug flow in hard walls (ref. 46) are also presented. Similar to Young and Crocker, Lester and Parott (ref. 48) have recently presented a Hermitian analysis for sound propagation in straight ducts with sound absorbing walls. Finite elements, Wiener Hopf, and wave propagation math models were found to give consistant results.

Irrotational Flow. Sigman, Majjigi and Zinn (ref. 20, item 7) presented the first finite element analysis which treated irrotational flows in ducts. They used a simple linear three node triangular element in conjunction with Galerkin analysis to model the sound propagation. The potential function wave equation is appropriate to inlet flow in a turbojet engine where the flow is nearly irrotational (excluding the boundary layer). The potential flow formulation gives an order of magnitude reduction in required core storage compared to the more general flow solutions to be presented next. As an illustrative example in their paper, they analyzed the hard wall version of the NASA QCSEE (quiet, clean short-haul experimental engine) inlet. This inlet was designed to suppress inlet-emitted engine machinery noise using a high throat Mach number and thus has somewhat more curvature than a conventional inlet. For an initial plane wave, their finite element analysis showed that significant distortion of the initial plane wave occurred due to the entrance curvature effects.

Majjigi, Sigman, and Zinn (refs. 49 and 50, item 8) have expanded their original analysis to include sound absorbing material by using a quadratic interpolation function. Using this program, Baumeister and Majjigi (ref. 51, item 8) estimated the sensitivity of duct attenuation to inlet curvature, centerbody and irrotational flow gradients for a high Mach number turbojet inlet. They showed that area variations can significiantly change the calculated attenuation as compared to the circular cylinder model presently being used for the design of such inlets.

The assumption of irrotationality eliminates the practical case of parallel shear boundary layer flow. Baumeister and Majjigi (ref. 51) showed that even in an approximate manner the velocity potential cannot be used to estimate the effects of sheared flow. However, a boundary layer correction based on the Goldstein-Rice analysis (ref. 52) was suggested for predicting the attenuation with shear in a soft wall duct.

Tag and Lumsdaine (ref. 53, item 9) also performed a similar irrotational analysis for a hard wall inlet using an isoparametric quadrilateral element. They showed that the finite element analysis can conveniently handle the problem of cutoff in a variable area duct. For a sample inlet, they also performed calculations to show the effects of duct geometry on far field attenuation and of flow gradients on the effective sound wavelength.

General Flow Field. Items 10, 11, and 12 in Table I are concerned with formulating a general finite element solution of the complete acoustic flow field, Eqs. (5-8). In most cases, the general theory has been applied to some relatively simple cases to check the theory.

Quinn (ref. 30, item 10) examined the use of various interpolation functions and finite element methods on many sample problems. He compared the accuracy of linear interpolation functions on triangles, bilinear interpolation function on rectangles and biquadratic interpolation functions on rectangles. He found that the biquadratics permit good approximation of curved boundaries and better convergence than the bilinear interpolation functions.

Abrahamson (refs. 54-56, item 11) has developed a finite element model using a linear rectangular element along with the Galerkin method. He has applied the method to conical horns, liners with axial impedance variations and the optimization of liners for maximum acoustic attenuation. He has devoted considerable effort (ref. 56) to reducing the computational times for large complex problems.

Astley, Eversman, and Thanh (refs. 57-60, item 12) have developed a finite element method based on weighted residuals using an eight node isoparametric element. As in Ref. 30, they also found the Galerkin method to be superior to the least squares approach. For uniform rectangular and circular ducts, they showed that the finite element method produces results for eigenvalues and transmission coefficients nearly identical to those from analytical approaches. Eversman, Astely and Thanh (ref. 57) also used the finite element method to explore the choking that might occur in a subsonic flow. They found that a large transmission loss is not an automatic consequence of propagation against a high subsonic mean flow.

NASA Lewis Research Center has begun an experimental program to check the results of the finite element models against experiment. A 0.5 area contraction in the form of a quartic curve has been constructed in which experimental results are currently being obtained. Figure 6 shows the comparison of the Astley-Eversman finite element program with the experimental data. As seen in Fig. 6, experiment and theory are in good agreement. The finite difference theory (dashed line) by Prof. James White will

be discussed later in the section on transient solutions to the wave equation.

SPECIAL NUMERICAL TRANSFORMATIONS

In the inlet to a turbojet engine, the dimensionless frequencies η are of order 30 to 50 for the higher harmonics of the blade passing frequency. The storage requirement and associated running times for these high frequencies are not practical at the present time. Some special techniques have been developed in order to reduce the storage requirements.

Wave Envelope Technique

To remove some (if not all) of the axially oscillatory part of the wave pressure profile and thereby greatly reduce the required number of grid points, Baumeister (refs. 61 and 62) assumes

$$p(x,y) = p_o(x,y)e^{-i2\pi x/\lambda} \tag{61}$$

where p represents the pressure of the oscillating curve in Fig. 7 and p_o represents the pressure of the wave envelope shown by the dashed line. The length λ represents the effective axial wave length of the oscillation. In general, λ is chosen to be the value associated with a particular mode propagating through a hard wall duct. For the case of a plane wave propagating in a soft wall duct without flow, λ is approximated by $1/\eta$. Substituting Eq. (61) into the Helmholtz Eq. (34) yields the wave envelope equation

$$\frac{\partial^2 p_o}{\partial x^2} + \frac{\partial^2 p_o}{\partial y^2} - i4\pi\eta\frac{\partial p_o}{\partial x} = 0 \tag{62}$$

The finite difference form of this equation was then programmed (ref. 60). Excellent agreement between the analytical and wave envelope finite difference calculations are shown in Fig. 8. For the $\eta = 5$, $L^*/H^* = 6$ case in Fig. 8, the conventional finite difference theory required 3600 grid points, whereas the wave envelope difference theory required only 100 grid points. Thus, a savings of 3500 grid points over the conventional difference theory was obtained. In Ref. 63, this technique was used to optimize multi-element liners of long lengths at high frequencies. This technique can also be used with finite elements.

At the present time, this technique has been applied only to the simple cases of no flow and plug flow. For a variable area duct with flow, it will be necessary to have λ a function of x. Calculated trial values of λ could be obtained from a one-dimensional solution of the governing equations.

Marching Techniques

Although initial value numerical solutions of elliptic equations are generally unstable (ref. 64, p. 63), Baumeister (refs. 65 and 66), using the Von Neumann stability analysis, showed that the two-dimensional Helmholtz wave equation can be solved approximately using explicit marching techniques. However, the grid spacing in the transverse y direction must be sufficiently large so that non-propagating acoustic modes cannot be resolved, that is,

$$\Delta y > \frac{0.32}{\eta} \tag{63}$$

Compared to standard finite-difference or finite-element boundary value approaches, the numerical marching technique is orders of magnitude shorter in computational time and required computer storage. This technique is limited, however, to high frequencies and to cases where reflections are small.

The numerical optimum attentuations were calculated using the marching technique and compared to the corresponding analytical results similar to Fig. 8. For dimensionless frequencies $\eta = 1$ or $\eta = 2$, the numerical results were in poor agreement, while for $\eta = 5$ or greater the method worked quite well. Consequently, marching could be used in conjunction with conventional analysis to handle the special cases of high frequency and long length.

Far Field Coupling

To obtain the far field acoustic radiation patterns and to eliminate the necessity of specifying the impedance of the duct at its exit, finite elements can be extended from the internal portion of a duct into the far field, as shown by Kagawa et al. (ref. 40, fig. 16). In Ref. 40, an acoustic horn with an opening into a semi-infinite space was analyzed by introducing a hypothetical spherical boundary with a characteristics $\rho_o c_o$ exit impedance termination. However, when taking account of acoustic radiation in this way, a spherical boundary of large area must be considered, which correspondingly results in solving a large matrix equation. To eliminate this large matrix requirement, Kagawa et al. (ref. 67) recently developed a combination of the finite element (in duct) and analytical methods (Green-Theorm - far field) to analyze sound propagation from an acoustic horn. Experiment and theory were found to be in good agreement.

Baumeister and Majjigi (ref. 51) presented a matrix partitioning approach that separated the duct and far field into two or more regions. The regions are coupled by an assumed value of impedance. For the no flow case in the far field, the dimensionless impedance can be chosen to be unity at a spherical surface. In Ref. 51, large matrix storage reductions (factor of 50) were obtained. For cases where complex flows occur around the exit, the first partition should be in the far field where an analytical value of impedance can be reasonably specified.

TRANSIENT NUMERICAL SOLUTIONS

In order to eliminate the storage requirements associated with the steady state numerical analysis of sound propagation in a turbojet engine inlet, Baumeister developed time dependent numerical solutions for noise propagation in a two-dimensional duct without flow (ref. 27), with parallel shear flow (ref. 68), and with axisymmetric plug flow (ref. 69). Advantageously, matrix storage requirements are completely eliminated in the time dependent analysis. The solution vectors for pressure and velocity need only be stored.

Difference Equations

The analysis begins with a noise source radiating into an initially quiescent duct. Next, an explicit iteration method obtains the transient as well as the "steady" state solution.

To illustrate how the transient equations are programmed consider the no flow cartesian wave equation (eq. (29) with $U_o = 0$) in one space dimension:

$$n^2 \frac{\partial^2 p}{\partial t^2} = \frac{\partial^2 p}{\partial x^2} \tag{64}$$

Away from the boundaries, the second derivatives in the wave equation can be represented by the usual central differences in time (subscript k) and space (subscripts i,j)

$$n^2 \left(\frac{P_i^{k+1} - 2P_i^k + P_i^{k-1}}{\Delta t^2} \right) = \left(\frac{P_{i+1}^k - 2P_i^k + P_{i-1}^k}{\Delta x^2} \right) \tag{65}$$

where Δt and Δx are the time and space mesh spacing, respectively. Solving Eq. (65) for P_i^{k+1} yields

$$P_i^{k+1} = 2P_i^k - P_i^{k-1} + \left(\frac{\Delta t}{n \Delta x} \right)^2 \left(P_{i+1}^k - 2P_i^k + P_{i-1}^k \right) \tag{66}$$

The procedure is explicit since all the past values of P^k are known as the new values of P^{k+1} are computed. The derivation with two space dimensions and boundary conditions is fully documented in Refs. 27, 68, and 69. Since Eq. (66) is a simple algebraic equation, storage is only required for the solution vectors P_i^k, P_i^{k-1}; that is, no matrix storage or manipulation is required. This was extremely useful in Ref. 68, where a simultaneous solution of the continuity and momentum equations was employed to obtain the acoustic values of P, U, and V.

Graphical Output

Fortunately, the pressure calculated at each instant of time need not be saved or displayed. Although multiple values of pressure are calculated, only the latest values (k,k-1) need be stored. After steady state is reached (checked numerially), the time-dependent results will be compared to the "steady" state results simply by dividing by $e^{i2\pi t}$, that is

$$p(x,y) = \frac{P(x,y,t)}{e^{i2\pi t}} \tag{67}$$

In this case where the source is a simple harmonic function of time $e^{i2\pi t}$, p represents the Fourier transform of $P(x,y,t)$ (ref. 18, p. 11). In this manner, the numerical results (refs. 27 and 69) are nearly identical to those shown in Fig. 4. The bookkeeping and graphical output is held to a minimum by the use of Eq. (67). The time-dependent analysis is considerably faster than the steady analysis, as seen in Fig. 9. In general, however, the computational time associated with the steady and transient analysis will be comparible. The major advantage of the transient analysis remains the elimination of matrix storage requirements. Because manipulation of matrices is omitted, the time dependent approach is much easier to program and debug.

Stability

Time-dependent numerical techniques have been applied to one-dimensional sound propagation (ref. 70, p. 258), two-dimensional vibration problems (ref. 32, p. 452), and the more general problem of compressible fluid flow (ref. 71). Numerical stability is a major difficulty associated with all these time dependent solutions. The new problem associated with two-dimensional soft wall acoustic problems is the influence of the boundary conditions on stability. The manner in which the boundary conditions are posed can cause the solution to be absolutely unstable (ref. 69). At the present time, the time marching technique has been found to be stable for no flow (ref. 27), plug flow (ref. 68), and axis symmetric spinning wave acoustics in a cylindrical duct (ref. 69). Numerical experimentation will be required to determine if the equations will remain stable and model the acoustic propagation when axial and transverse variations in the mean flow are considered.

At the present time, the transient method appears to have one major drawback. The transient method does not converge for cut-off modes (ref. 69). This has implications as to its use in a variable area where modes may become cut-off in the small area portion of the duct. This will ultimately have to be resolved since cut-off modes will be encountered in real problems. In the mean time, the steady state numerical techniques can be conveniently employed near cut-off. Because of the relatively long axial wavelength of a near cut-off mode, the required number of grid points (or elements) is relatively small.

Variable Area

The finite element method is inappropriate for the two-dimensional transient problems because the solutions are implicit requiring storage of the usual large matrix. Therefore, in applying the transient method to problems with area variations, the method of mapping in conjunction with the finite difference method could be used.

In particular, the mapping procedure developed by Thompson et al. (ref. 72) provides for the automatic generation of a general coordinate system with coordinate lines coincident with all the boundaries of an arbitrary shaped duct. Professor James White of the University of Tennessee (Knoxville) under NASA grant NAG 3-18, is extending the procedure of Ref. 72 to the problem of sound propagation in variable area ducts. In a form similar to Eq. (59), Professor White has developed the appropriate transformed acoustic equations which are solved in the mapped rectangular domain. The results are then transformed back into the physical plane by an inverse mapping procedure.

Figure 6 shows a comparison of Professor White's transient finite analysis with the experimental data for the quartic duct discussed earlier in conjunction with the Astley-Eversman finite element analysis. As seen in Fig. 6, experiment and theory are in good agreement.

CONCLUDING REMARKS

The finite difference and finite element theories have proven to be useful calculational tools in handling acoustic propagation in ducts with discontinuities in lining impedance, with area variations, and in ducts where large variations in the mean flow field occur.

At the present time, the steady and transient numerical theories are capable of handling the design of mufflers, expansion chambers, and exhaust ducts of turbofan engines where the effective frequency n is quite small. In contrast, the steady numerical theories are not as yet capable of analyzing a practical turbofan inlet because of the high frequencies and Mach numbers in the inlet. Special steady state transformations and the transient technique have potential for handling this problem.

At the present time, NASA, universities and industry are extending the steady and transient numerical techniques to situations involving high frequencies, high Mach numbers and geometries with large area variations. The transient numerical technique is being adapted to handle nonlinear effects including acoustic shocks. An additional goal is to develop more realistic inlet and exit conditions to model a typical turbofan aircraft nacelle.

REFERENCES

1 Craggs, A., "The Use of Simple Three-Dimensional Acoustic Finite Elements For Determining the Natural Modes and Frequencies of Complex Shaped Enclosures," Journal of Sound and Vibration, Vol. 23, No. 3, 1972, pp. 331-339.

2 Shuku, T. and Ishihara, K., "The Analysis of the Acoustic Field in Irregularly Shaped Rooms by the Finite Element Method," Journal of Sound and Vibration, Vol. 29, No. 1, 1973, pp. 67-76.

3 Petyt, M., Lea, J., and Koopmann, C. H., "A Finite Element Method for Determining the Acoustic Modes of Irregular Shaped Cavities," Journal of Sound and Vibration, Vol. 45, No. 4, 1976, pp. 495-502.

4 Joppa, P. D. and Fyfe, I. M., "A Finite Element Analysis of the Impedance Properties of Irregular Shaped Cavities with Absorptive Boundaries," Journal of Sound and Vibration, Vol. 56, No. 1, 1978, pp. 61-69.

5 Nefske, D. J. and Howell, L. J., "Automobile Interior Noise Reduction Using Finite Element Methods," SAE Paper No. 780365, Feb. 1978.

6 Richards, T. L. and Jha, S. K., "A Simplified Finite Element Method for Studying Acoustic Characteristics Inside a Car Cavity," Journal of Sound and Vibration, Vol. 63, No. 1, 1979, pp. 61-72.

7 Unruh, J. F., "A Finite Element Subvolume Technique for Structural-Borne Interior Noise Prediction," AIAA Paper 79-0585, Mar. 1979.

8 van Nieuwland, J. M. and Weber, C., "Eigenmodes in Nonrectangular Reverberation Rooms," Noise Control Engineering, Vol. 13, No. 3, Nov.-Dec., 1979, pp. 112-120.

9 Gladwell, G. M. L. and Mason, V., "Variational Finite Element Calculation of the Acoustic Response of a Rectangular Panel," Journal of Sound and Vibration, Vol. 14, No. 1, 1971, pp. 115-135.

10 Craggs, A., "The Transient Response of a Coupled Plate-Acoustic System Using Plate and Acoustic Finite Elements," Journal of Sound and Vibration, Vol. 15, No. 4, 1971, pp. 509-528.

11 Craggs, A. and Stead, G., "Sound Transmission Between Enclosures - A Study Using Plate and Acoustic Finite Elements," Acoustica, Vol. 35, No. 2, 1974, pp. 89-98.

12 Kagawa, Y., et al., "A Finite Element Approach to a Coupled Structural-Acoustic Radiation System With Application to Loudspeaker Characteristic Calculation," Journal of Sound and Vibration, Vol. 69, No. 2, 1980, pp. 229-243.

13 Wynne, C. A. and Plumblee, H. E., "Calculation of Eigenvalues of the Finite Difference Equations Describing Sound Propagation in a Duct Carrying Sheared Flow," Presented at the 79th Meeting of the Acoustical Society of America, Atlantic City, New Jersey, April 1970. See Journal of the Acoustical Society of America, Vol. 48, No. 1, 1970, Abstract D11, p. 76.

14 Watson, W. R., "A Finite Element Analysis of Sound Propagation in a Rectangular Duct of Finite Length With Peripherally Variable Liners," AIAA Paper No. 77-1300, Oct. 1977.

15 Astley, R. J. and Eversman, W , "A Finite Element Formulation of the Eigenvalue Problem in Lined Ducts with Flow," Journal of Sound and Vibration, Vol. 65, No. 1, 1979, pp. 61-74.

16 Dong, S. B. and Liu, C. Y., "A Finite-Element Analysis of Sound Propagation in a Nonuniform Moving Medium," Journal of the Acoustical Society of America, Vol. 66, No. 2, Aug. 1979, pp. 548-555.

17 Astley, R. J. and Eversman, W., "The Finite Element Duct Eigenvalue Problem: An Improved Formulation with Hermitian Elements and No-Flow Condensation," Journal of Sound and Vibration, Vol. 69, No. 1, 1980, pp. 13-25.

18 Goldstein, M. E., Aeroacoustics, McGraw-Hill, New York, 1976.

19 Savkar, S. D., "Propagation of Sound in Ducts With Shear Flow," Journal of Sound and Vibration, Vol. 19, No. 3, 1971, pp. 355-372.

20 Sigman, R. K., Majjigi, R. K., and Zinn, B. T., "Determination of Turbofan Inlet Acoustics Using Finite Elements," American Institute of Aeronautics and Astronautics Journal, Vol. 16, No. 11, 1978, pp. 1139-1145.

21 Morse, P. M. and Ingard, K. U., Theoretical Acoustics, McGraw-Hill, New York, 1968.

22 Eversman, W., Astley, R. J., and Thanh, V. P., "Transmission in Non-uniform Ducts - A Comparative Evaluation of Finite Element and Weighted Residuals Computational Schemes," AIAA Paper No. 77-1299, Oct. 1977.

23 Tag, I. A. and Lumsdaine, E., "An Efficient Finite Element Technique for Sound Propagation in Axisymmetric Hard Wall Ducts Carrying High Subsonic Mach Number Flows," AIAA Paper No. 78-1154, July 1978.

24 Alfredson, R. J., "A Note on the Use of the Finite Difference Method for Predicting Steady State Sound Fields," Acoustica, Vol. 28, No. 5, May 1973, pp. 296-301.

25 Baumeister, K. J. and Bittner, E. C., "Numerical Simulation of Noise Propagation in Jet Engine Ducts," NASA TN D-7339, 1973.

26 Baumeister, K. J. and Rice, E. J., "A Difference Theory for Noise Propagation in an Acoustically Lined Duct with Mean Flow," Aeroacoustics: Jet and Combustion Noise; Duct Acoustics, H. T. Nagamatsu, J. V. O'Keefe, and I. R. Schwartz, eds., Progress in Astronautics and Aeronautics Series, Vol. 37, American Institue of Aeronautics and Astronautics, New York, 1975, pp. 435-453.

27 Baumeister, K. J., "Time Dependent Difference Theory for Noise Propagation in Jet Engine Ducts," AIAA Paper No. 80-0098, Jan. 1980.

28 Baumeister, K. J., "Finite-Difference Theory for Sound Propagation in a Liner Duct with Uniform Flow Using the Wave Envelope Concept," NASA TP-1001, 1977.

29 Quinn, D. W., "The Analysis of Sound Propagation in Jet Engine Ducts Using the Finite Difference Method," AFFDL-TR-79-3063, Air Force Flight Dynamics Lab., Wright-Patterson AFB, Ohio, June 1979. (AD-A074233.)

30 Quinn, D. W., "A Finite Element Method for Computing Sound Propagation in Ducts Containing Flow," AIAA Paper No. 79-0661, Mar. 1979.

31 Beaubien, M. J. and Wexler, A., "Interative, Finite Difference Solution of Interior Eigenvalues and Eigenfunctions of Laplace's Operator," Computer Journal, Vol. 14, Aug. 1971, pp. 263-269.

32 Gerald, C. F., Applied Numerical Analysis, 2nd ed., Addison-Wesley, Reading, MA. 1978.

33 Quinn, D. W., "A Finite Difference Method for Computing Sound Propagation in Nonuniform Ducts," AIAA Paper No. 75-130, Jan. 1975.

34 Quinn, D. W., "Attenuation of Sound Associated with a Plane Wave in a Multi-sectional Duct," in Aeroacoustics: Fan Noise and Control; Duct Acoustics; Rotor Noise, I. R. Schwartz, H. T. Nagamatsu, and W. Strahle, eds, Progress in Astronautics and Aeronautics Series, Vol. 44, American Institute of Aeronautics and Astronautics, New York, 1976, pp. 331-345.

35 Chen, L. T. and Caughey, D. A., "Calculation of Transonic Inlet Flowfields Using Generalized Coordinates, AIAA 79-0012, Jan. 1979.

36 Young, C.-I. J. and Crocker, M. J., "Prediction of Transmission Loss in Mufflers by the Finite-Element Method," Journal of the Acoustical Society of America, Vol. 57, No. 1, Jan. 1975, pp. 144-148.

37 Kapur, A. and Mungur, P., "Duct Acoustics and Acoustic Finite Element Method," Aeroacoustics: Fan Noise and Control; Duct Acoustics; Rotor Noise, I. R. Schwartz, H. T. Nagamatsu, and W. Strahle, eds., Progress in Astronautics and Aeronautics, Vol. 44, American Institute of Aeronautics and Astronautics, New York, 1976, pp. 363-370.

38 Huebner, K. H., The Finite Element Method for Engineers, Wiley, New York, 1975.

39 McCracken, D. D. and Dorn, W. S., Numerical Methods and FORTRAN Programming, Wiley, New York, 1964.

40 Kagawa, Y. and Omote, T., "Finite-Element Simulation of Acoustic Filters of Arbitrary Profile with Circular Cross Section," Journal of the Acoustical Society of America, Vol. 60, No. 5, Nov. 1976, pp. 1003-1013.

41 Kagawa, Y., Yamabuchi, T., and Mori, A., "Finite Element Simulation of an Axisymmetric Acoustic Transmission System with a Sound Absorbing Wall," Journal of Sound and Vibration, Vol. 53, no. 3, 1977, pp. 357-374.

42 Craggs, A., "A Finite Element Method for Damped Acoustic Systems: An Application to Evaluate the Performance of Reactive Mufflers," Journal of Sound and Vibration, Vol. 48, No. 3, 1976, pp. 377-392.

43 Craggs, A., "A Finite Element Method for Modelling Dissipative Mufflers With a Locally Reactive Lining," Journal of Sound and Vibration, Vol. 54, No. 2, 1977, pp. 285-296.

44 Craggs, A., "A Finite Element Model for Rigid Porous Absorbing Materials," Journal of Sound and Vibration, Vol. 61, No. 1, 1978, pp. 101-111.

45 Craggs, A., "Coupling of Finite Element Acoustic Absorption Models," Journal of Sound and Vibration, Vol. 66, No. 4, 1979, pp. 605-613.

46 Tag, I. A. and Lumsdaine, E., "A Finite Element Approach to the Problem of Noise Propagation and Attenuation in Industrial Ducts," Fluid Transients and Acoustics in the Power Industry, ASME Winter Annual Meeting, G. V. Smith, ed., American Society of Mechanical Engineers, New York, 1978, pp. 317-323.

47 Tag, I. A. and Akin, J. E., "Finite Element Solution of Sound Propagation in a Variable Area Duct," AIAA Paper No. 79-0663, Mar. 1979.

48 Lester, H. C. and Parrott, T. L., "Application of Finite Element Methodology for Computing Grazing Incidence Wave Structure in an Impedance Tube: Comparison with Experiment," AIAA Paper No. 79-0664, Mar. 1979.

49 Majjigi, R. K., "Application of Finite Element Techniques in Predicting the Acoustic Properties of Turbofan Inlets," PhD. Thesis, Georgia Institute of Technology, Atlanta, 1979.

50 Majjigi, R. K., Sigman, R. K., and Zinn, B. T., "Wave Propagation in Ducts Using the Finite Element Method." AIAA Paper No. 79-0659, Mar. 1979.

51 Baumeister, K. J. and Majjigi, R. K., "Applications of the Velocity Potential Function to Acoustic Duct Propagation and Radiation from Inlets Using Finite Element Theory," AIAA Paper No. 79-0680, Mar. 1979.

52 Goldstein, M. and Rice, E., "Effect of Shear on Duct Wall Impedance," Journal of Sound and Vibration, Vol. 30, No. 1, Sep. 1973, pp. 79-84.

53 Tag, I. and Lumsdaine, E., "An Efficient Finite Element Technique for Sound Propagation in Axisymmetric Hard Wall Ducts Carrying High Subsonic

Mach Number Flows," AIAA Paper No. 78-1154, July 1978.

54 Abrahamson, A. L., "A Finite Element Algorithm for Sound Propagation in Axisymmetric Ducts Containing Compressible Mean Flow," RR-50624, Wyle Labs., Inc., Hampton, VA, June 1977. (NASA CR-145209.)

55 Abrahamson, A. L., "A Finite Element Algorithm for Sound Propagation in Axisymmetric Ducts Containing Mean Flow," AIAA Paper No. 77-1301, Oct. 1977.

56 Abrahamson, A. L., "Acoustic Duct Liner Optimization Using Finite Elements," AIAA Paper No. 79-0662, Mar. 1979.

57 Astley, R. J. and Eversman, W., "A Finite Element Method for Transmission in Non-Uniform Ducts Without Flow: Comparison with the Method of Weighted Residuals," Journal of Sound and Vibration, Vol. 57, No. 3, 1978, pp. 367-388.

58 Eversman, W., Astley, R. J., and Thanh, V. P., "Transmission in Nonuniform Ducts - A Comparative Evaluation of Finite Element and Weighted Residuals Computational Schemes," AIAA Paper No. 77-1299, Oct. 1977.

59 Astley, R. J. and Eversman, W., "The Application of Finite Element Techniques to Acoustic Transmission in Lined Ducts with Flow," AIAA Paper No. 79-0660, Mar. 1979.

60 Thanh, V. P., "Computational Methods for Sound Transmission in Nonuniform Wave-Guides," Ph.D. Thesis, University of Canterbury, Christchurch, New Zealand, June 1979.

61 Baumeister, K. J., "Analysis of Sound Propagation in Ducts Using the Wave Envelope Concept," NASA TN D-7719, 1974.

62 Baumeister, K. J., "Wave Envelope Analysis of Sound Propagation in Ducts with Variable Axial Impedance," Aeroacoustics: Fan Noise and Control; Duct Acoustics; Rotor Noise, I. R. Schwartz, H. T. Nagamatsu, and W. Strahle, eds., Progress in Astronautics and Aeronautics Series, Vol. 44, American Institute of Aeronautics and Astronautics, New York, 1976, pp. 451-474.

63 Baumeister, K. J. "Evaluation of Optimized Multisectioned Acoustic Liners," AIAA Journal, Vol. 17, No. 11, Nov. 1979, pp. 1185-1192.

64 Petrovskii, I. G., Lectures on Partial Differential Equations, A. Shenitzer, transl., Interscience, New York, 1954.

65 Baumeister, K. J., "Numerical Spatial Marching Techniques for Estimating Duct Attenuation and Source Pressure Profiles," 95th Meeting of the Acoustical Society of America, Providence, R.I., May 16-19, 1978 (also NASA TM-78857, 1978).

66 Baumeister, K. J., "Numerical Spatial Marching Techniques in Duct Acoustics," Journal of the Acoustical Society of America, Vol. 65, 1979, pp. 297-306.

67 Kagawa, Y., Yamabuchi, T., and Yoshikawa, T., "Finite Element Approach to Acoustic Transmission-Radiation Systems and Application to Horn and Silencer Design," Journal of Sound and Vibration, Vol. 69, No. 2, 1980, pp. 207-228.

68 Baumeister, K. J., "A Time Dependent Difference Theory for Sound Propagation in Ducts with Flow," 98th Meeting of the Acoustical Society of America, Salt Lake City, UT, 1979 (also NASA TM-79302, 1979).

69 Baumeister, K. J., "Time Dependent Difference Theory for Sound Propagation in Axisymmetric Ducts with Plug Flow, AIAA Paper No. 80-1017, June 1980.

70 Richtmyer, R. D. and Morton, K. W., Difference Methods for Initial-Valve Problems, 2nd ed., Interscience, New York, 1967.

71 Roache, P. J., Computational Fluid Dynamics, Hermosa, Alburquerque, N.M., 1972.

72 Thompson, J. F., Thames, F. C., and Mastin, C. W., "Automatic Numerical Generation of Body-Fitted Curvilinear Coordinate System for Field Containing Any Number of Arbitrary Two-Dimensional Bodies," Journal of Computational Physics, Vol. 15, 1974, pp. 299-319.

TABLE I. - FINITE ELEMENT SUMMARY

Item number	Element type	Interpolation function	Dependent variables	Finite element method	Types of acoustic propagation	References
1		Hermitian fourth order	$p, \frac{\partial p}{\partial x}, \frac{\partial p}{\partial y}$	Variational	No flow Hard wall	(36)
2		Linear ring	p	Variational	No flow Hard wall	(40)
3		Quadratic ring	p	Variational	No flow Soft wall	(41), (67)
4		Hexahedral isoparametric	p	Variational	No flow Soft walls Non-local	(42), (43), (44) (45)
5		Linear isoparametric	p	Variational	No flow (plug)	(46), (47)
6		Hermitian fourth order	$p, \frac{\partial p}{\partial x}, \frac{\partial p}{\partial y}, \frac{\partial^2 p}{\partial x \partial y}$	Galerkin	No flow Soft walls	(48)
7		Linear	ϕ	Galerkin	Irrotational Hard walls	(20)
8		Quadratic	ϕ	Galerkin	Irrotational Soft walls	(49), (50), (51)
9		Linear isoparametric	ϕ	Galerkin	Irrotational Hard walls	(53)
10		Linear quadratic isoparametric	p, u, v	Least squares Galerkin	General flow	(30)
11		Linear	p, u, v, w	Galerkin	General flow	(54), (55), (56)
12		Quadratic isoparametric	p, u, v	Least squares Galerkin	General flow	(57), (58), (59), (60)

ORIGINAL PAGE IS
OF POOR QUALITY

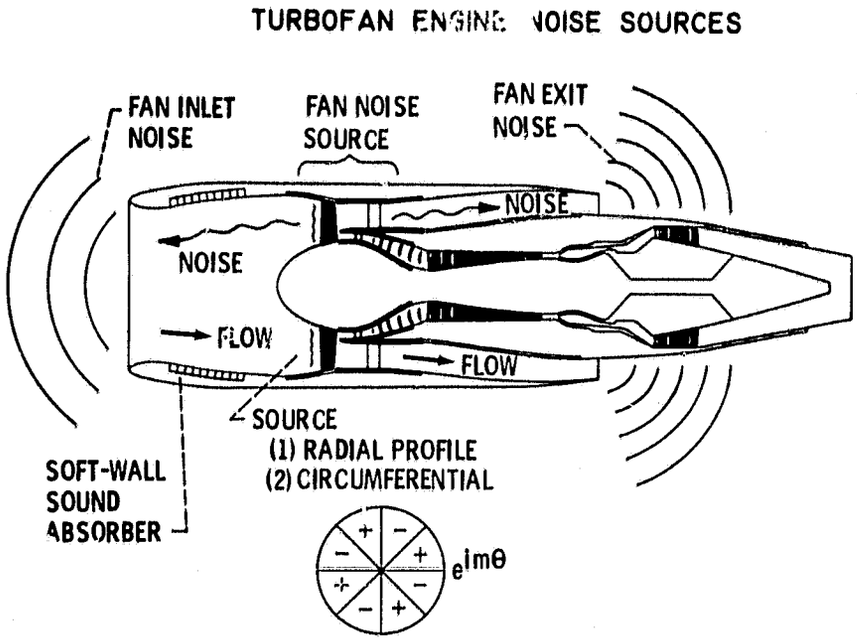

Figure 1. - Duct structure for turbofan engine.

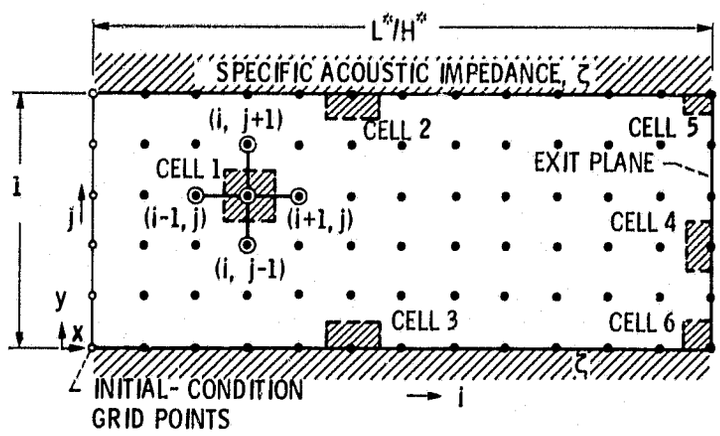

Figure 2. - Coordinate and grid-point representation of two-dimensional, soft-wall duct.

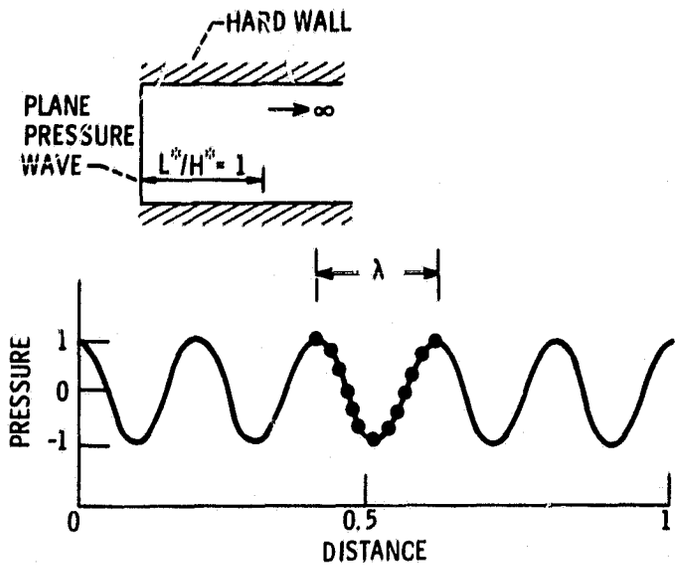

Figure 3. - Pressure profile (real part) in a hard wall duct for $\eta = 5$, $L^*/H^* = 1$.

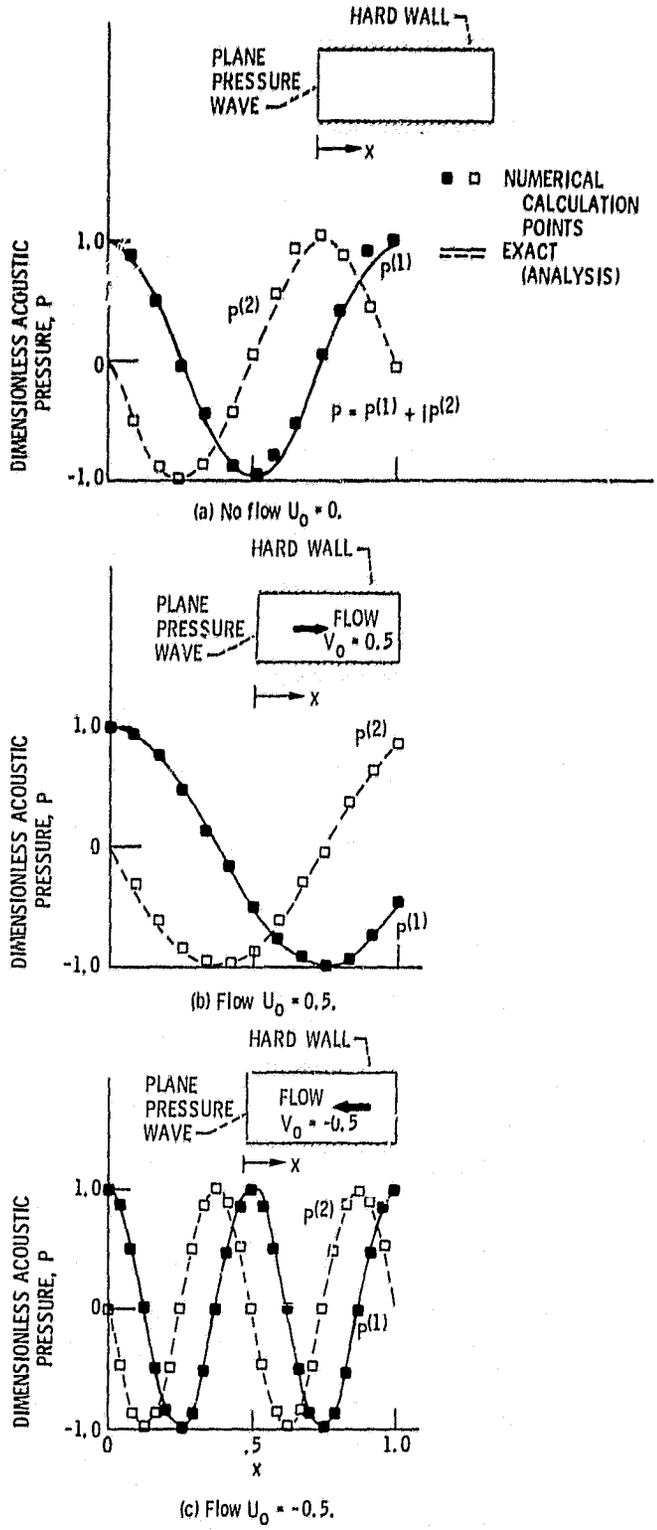

Figure 4. - Analytical and numerical pressure profiles for sound propagation in hard wall ducts for $\eta = 1$. $L''/H'' = 1$ and Mach numbers as shown.

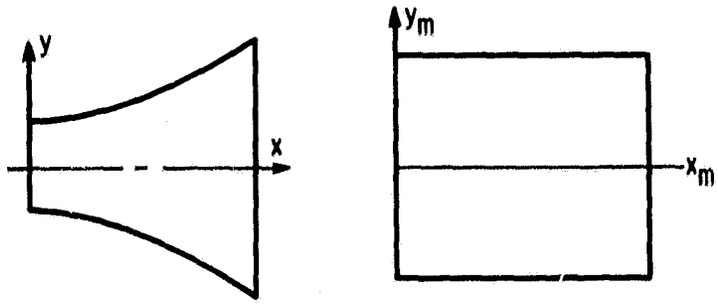

(a) Real plane. (b) Transformed plane.

Figure 5. - Conformal map of Hyperbolic Horn into a rectangular duct.

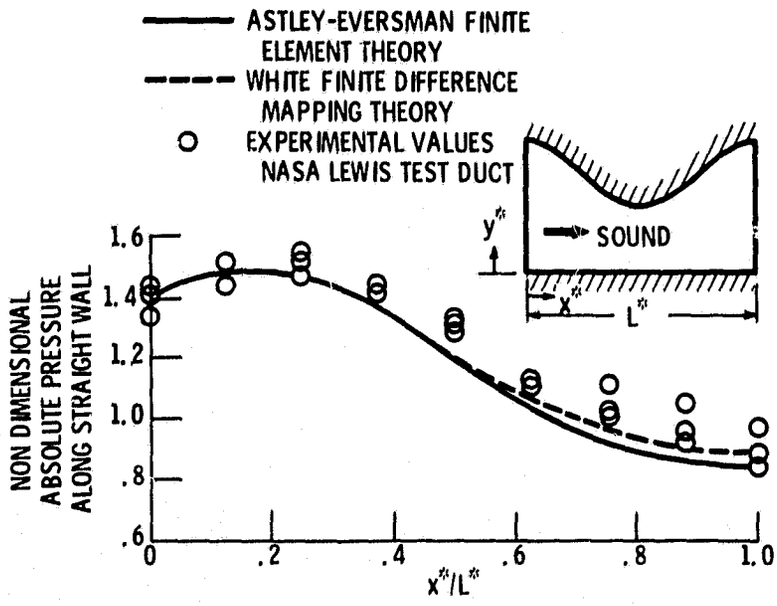

Figure 6. - Comparison of Astley-Eversman finite element theory and White finite difference mapping theory to experiment (η = 0.172).

ORIGINAL PAGE IS
OF POOR QUALITY

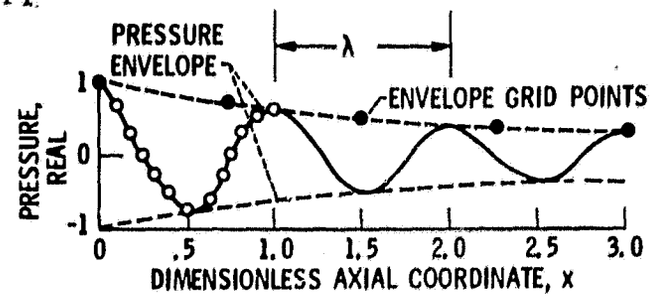

Figure 7. - Illustration of Wave Envelope method in determining the pressure profile for sound propagation in a soft-wall duct for dimensionless frequency $\eta = 1$ and duct length $L^*/H^* = 3$.

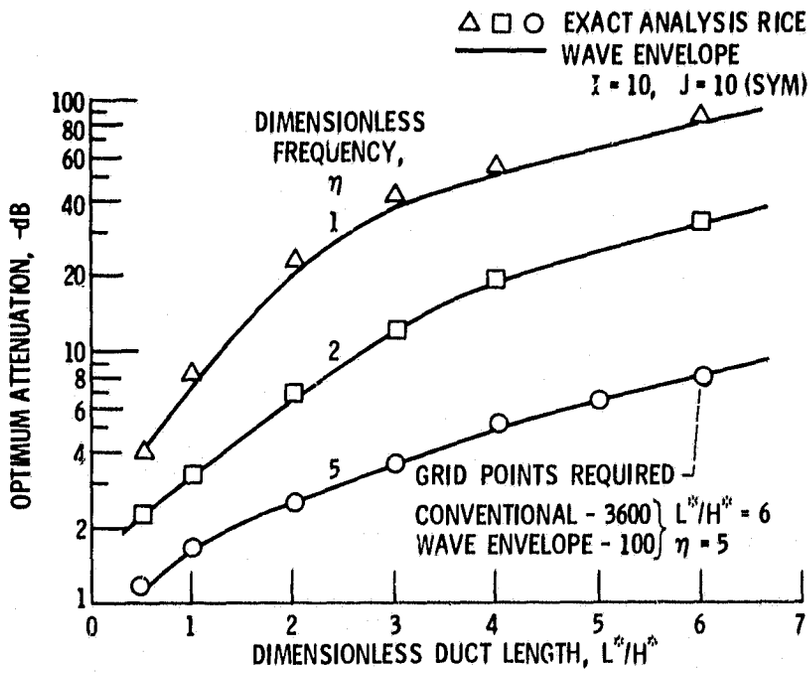

Figure 8. - Wave envelope solution for optimum (maximum possible) attenuation in a two-dimensional soft wall duct without flow and plane wave input.

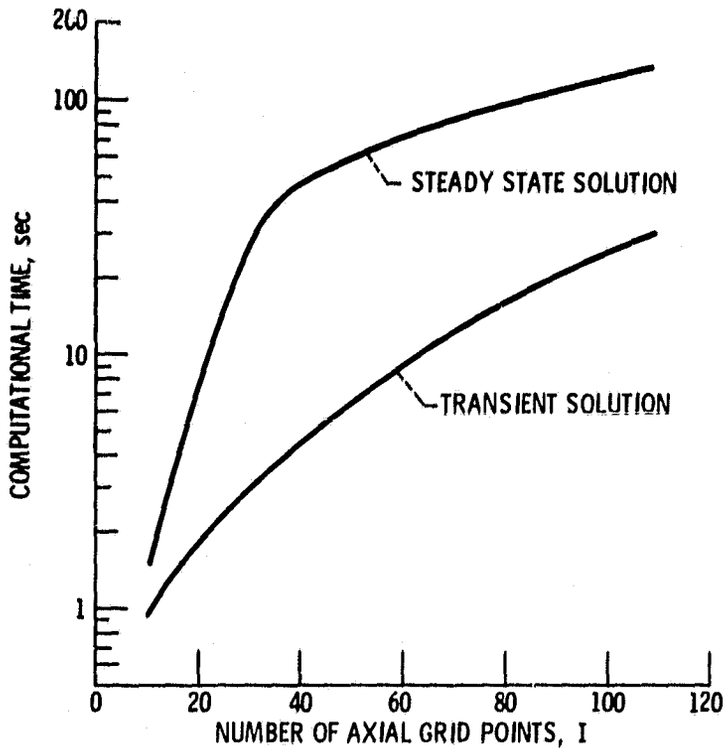

Figure 9. - Comparison of transient and steady state calculations for plane wave propagation in a hard wall duct ($\eta = 1$, $L^*/H^* = 1$, $J = 20$).

1. Report No.	2. Government Accession No.	3. Recipient's Catalog No
NASA TM-81553		

4. Title and Subtitle	5. Report Date
NUMERICAL TECHNIQUES IN LINEAR DUCT ACOUSTICS - A STATUS REPORT	6. Performing Organization Code
7. Author(s) K. J. Baumeister	8. Performing Organization Report No E-513
9. Performing Organization Name and Address National Aeronautics and Space Administration Lewis Research Center Cleveland, Ohio 44135	10. Work Unit No.
	11. Contract or Grant No.
12. Sponsoring Agency Name and Address National Aeronautics and Space Administration Washington, D.C. 20546	13. Type of Report and Period Covered Technical Memorandum
	14. Sponsoring Agency Code

15. Supplementary Notes

Prepared for the Winter Annual Meeting of the American Society of Mechanical Engineers, Chicago, Illinois, November 17-21, 1980.

16. Abstract

A review is presented covering both finite difference and finite element analysis of small amplitude (linear) sound propagation in straight and variable area ducts with flow, as might be found in a typical turbojet engine duct, muffler, or industrial ventilation system. Both "steady" state and transient theories are discussed. Emphasis is placed on the advantages and limitations associated with the various numerical techniques. Examples of practical problems are given for which the numerical techniques have been applied.

17. Key Words (Suggested by Author(s))	18. Distribution Statement
Sound; Muffler; Wave equation; Finite difference; Finite element	Unclassified - unlimited STAR Category 71

19. Security Classif. (of this report)	20. Security Classif. (of this page)	21. No. of Pages	22. Price*
Unclassified	Unclassified		

* For sale by the National Technical Information Service, Springfield, Virginia 22161

NASA-C-168 (Rev. 10-75)